JOURNAL OF MATERIALS SCIENCE 27 (1992) 4883–4889

Fracture behaviour of rubber-toughened polymer blends

E. J. MOSKALA
Eastman Chemical Company, PO Box 1972, Kingsport, TN 37662, USA

The fracture toughness of a core-shell rubber modified polycarbonate–copolyester blend was determined by using the *J*-integral approach. Single-edge notch bend specimens were tested at room temperature using a crosshead speed of 1 mm min^{-1}. The resistance curve for the blend was not affected by specimen width, direction of crack growth with respect to mould-flow direction, and sidegrooving. Fractographic analysis suggested that the matrix debonded from the rubber particles thus relieving the triaxial stresses and enabling the matrix to yield more easily. The initiation of crack growth in the *J*-tests was observed to occur shortly after the onset of non-linearity in the load–deflection curve. Consequently, an attempt was made to describe fracture in this blend by using linear elastic fracture mechanics.

1. Introduction

As polymeric materials are becoming more popular in load-bearing applications, it is necessary to have a thorough understanding of their ability to resist fracture. Linear elastic fracture mechanics (LEFM) has been used successfully to describe fracture in many brittle polymers [1, 2]. According to the principles of LEFM, fracture occurs when the magnitude of the stress intensity around the crack tip exceeds a critical value K_{1c}. Guidelines for determining K_{1c} are provided by the ASTM [3]. K_{1c} will be a valid plane strain parameter if the following size criteria are satisfied:

$$a_0,\ W - a_0,\ B \geqslant 2.5(K_{1c}/\sigma_y)^2$$

Where a_0 is the initial notch length, W is specimen width, B is specimen thickness, and σ_y is yield stress. These criteria ensure that the plastic zone which develops in the vicinity of the crack tip is small with respect to the dimensions of the specimen.

The toughness of brittle polymers can be enhanced by the addition of a rubbery phase [4]. However, it is often not possible to apply LEFM to the toughened materials because of their low yield stresses; the thicknesses which would be required to satisfy the criteria described above may be beyond the range of thicknesses which can be formed by standard processing techniques. In these situations the *J*-integral, an elastic–plastic parameter, may be used to characterize fracture toughness. The *J*-integral approach developed by Begley and Landes [5] provides a measure of fracture toughness, J_{1c}, which represents the energy required to initiate crack growth. According to ASTM Standard E-813-87 for *J*-testing of metallic materials [6], a valid value of J_{1c} is obtained when the following size criteria are satisfied:

$$B \text{ and } W\text{-}a_0 \geqslant 25J_{1c}/\sigma_y \quad (1)$$

These criteria produce plastic plane strain stress conditions at the crack front and allow for the use of significantly smaller specimen dimensions than are required for LEFM testing.

The *J*-integral approach has been used to characterize the fracture toughness of several toughened plastics including an acrylonitrile-butadiene-styrene blend [7–9], toughened semicrystalline nylon 6,6 [7–10], toughened PVC [8, 9, 11], impact-modified poly (butylene terephthlate) –polycarbonate blends [7], and core-shell rubber modified polycarbonate [12]. It was reported that crack growth in most of these materials initiated shortly after the onset of non-linearity in the load–deflection curves [7, 8]. This suggests that crack initiation in toughened blends may possibly be described by an LEFM approach. The objectives of this work were (1) to evaluate the fracture toughness of a toughened polycarbonate–copolyester blend by using the *J*-integral method, (2) to determine the toughening mechanism at work in this blend, and (3) to determine the extent to which LEFM can describe fracture in toughened plastics.

2. Experimental procedure

A blend of polycarbonate and a copolyester of terephthalic acid, ethylene glycol, and 1,6-cyclohexanedimethanol was toughened with a core-shell impact modifier consisting of a glassy shell and a rubbery core. The particle size of the impact modifer was approximately 0.3 μm. Plaques with dimensions 6.3 mm × 127 mm × 127 mm were injection moulded. Single-edge notch bend (SENB) specimens were machined from the plaques so that the thickness of the specimens corresponded to the thickness of the plaques. The width of the specimens was varied from 12.7 mm to 25.4 mm. The specimens were notched with a single-point flycutter. The notch was subsequently sharpened by sliding a razor blade across the root of the machined notch. At least two days passed before the fracture tests were performed to

0022–2461

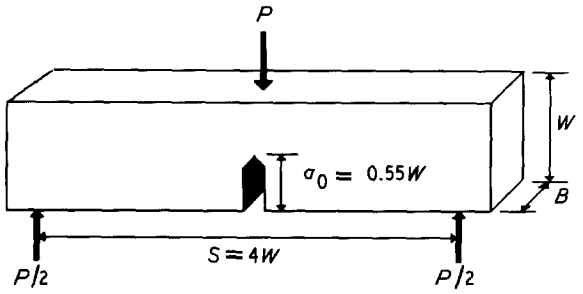

Figure 1 Schematic of the single-edge notch bend (SENB) specimen geometry.

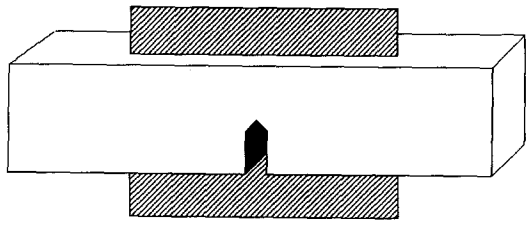

Figure 2 Schematic of a sectioned SENB specimen.

permit stress relaxation at the crack tip. The ratio of the initial notch length-to-specimen width, a_0/W, was 0.55. A diagram of the SENB specimen is shown in Fig. 1.

The J-integral was determined using a multiple specimen resistance-curve (R-curve) method developed by the European Group on Fracture Task Group on Polymers [13]. This method is similar to ASTM Standard E-813-87 with some modifications for plastic materials. A series of identical specimens were loaded to different displacements by using a cross-head rate of 1 mm min^{-1} and a span-to-specimen width ratio, S/W, of 4. Displacement was measured with the internal transducer of the testing machine. After rapid unloading, the specimens were cooled in liquid nitrogen for a minimum of 5 min and then placed back on the loading rig and broken open by using a crosshead speed of 500 mm min^{-1}. Crack growth, Δa, was measured from the exposed fracture surfaces by using a travelling microscope. J was calculated using the following expression:

$$J = 2U/B(W\text{-}a_0)$$

where U, energy, is the area under the load versus displacement curve. A plot of J versus Δa was constructed and a best fit curve, with the form of a simple power law given by

$$J = A\Delta a^D$$

where A and D are constants, was drawn through the data. The initiation toughness, J_{Ic}, was evaluated by using the blunting line construction. The blunting line takes into account crack extension due to crack tip blunting and is given by

$$J = 2\sigma_y\Delta a$$

J_{Ic} is taken as the value of J where the resistance curve intersects a line parallel to the blunting line and offset from the origin by 0.2 mm.

Fracture surfaces were examined by optical microscopy (OM) by using a Wild M400 optical microscope and by scanning electron microscopy (SEM) by using a Cambridge Instruments Stereoscan 200 scanning electron microscope. Specimens were coated with a thin layer of gold in a sputtering chamber before the SEM observations.

It will be shown that the length of the plastic zone ahead of the crack tip can be easily measured from the fracture surface by optical microscopy. However, no information concerning the depth of the plastic zone can be obtained from the fracture surface. To analyse this feature, several specimens were not broken open after testing, but instead were sectioned according to the diagram shown in Fig. 2. This produced a side view of the propagating crack and plastic zone in the vicinity of the crack tip. The inner surfaces of the sectioned specimens were polished with 600 grit paper and examined by OM with reflected light. Also, thin sections were microtomed from the inner surfaces of the sectioned specimens and examined by OM with transmitted light.

3. Results and discussion

A typical load–deflection curve for SENB specimens with width equal to 19.6 mm is shown in Fig. 3. The points at which the different specimens were unloaded and the amounts of crack growth incurred are indicated in the figure. Crack initiation occurs shortly after the onset of non-linearity, suggesting that an LEFM parameter may be used to characterize crack initiation. This possibility will be discussed in a subsequent section. Load–deflection diagrams of specimens with widths equal to 12.5 mm and 25.4 mm showed similar features. J–Δa data for each specimen width are shown in Fig. 4. As can be seen, specimen width has no effect on the resistance curve. J_{Ic} for the toughened blend is 10.8 kJ m^{-2}. This value satisfies the criteria given by Equation 1.

Yee *et al.* [12] and Narisawa and Takemori [7] determined J_{Ic} in core-shell rubber modified polycarbonate and impact-modified poly(butylene terephthalate)–polycarbonate blends, respectively, by using ASTM Standard E-813-81 [14]. Since these materials are similar to the toughened copolyester–polycarbonate blend used in this work, it is worthwhile to evaluate J_{Ic} by using the same version of the ASTM procedure. In ASTM Standard E-813-81 an R-curve is defined by a linear regression line through data bounded by offset exclusion lines at 0.6% and 6% of the uncracked ligament, $W\text{-}a_0$. J_{Ic} is taken as the intersection of the R-curve with the blunting line. Fig. 5 shows the R-curve determined using this procedure (specimen width equals 19.6 mm). A J_{Ic} value of 4.9 kJ m^{-2} is obtained. Yee *et al.* [12] and Narisawa and Takemori [7] obtained J_{Ic} values of 5–6 kJ m^{-2} and 3–4 kJ m^{-2}, respectively. It should be noted that the EGF protocol, which is based on ASTM Standard E-813-87, gives a higher value of J_{Ic} than ASTM Standard E-813-81. This is to be expected since the EGF protocol uses an offset blunting line to determine J_{Ic}. The difference between the J_{Ic} values determined

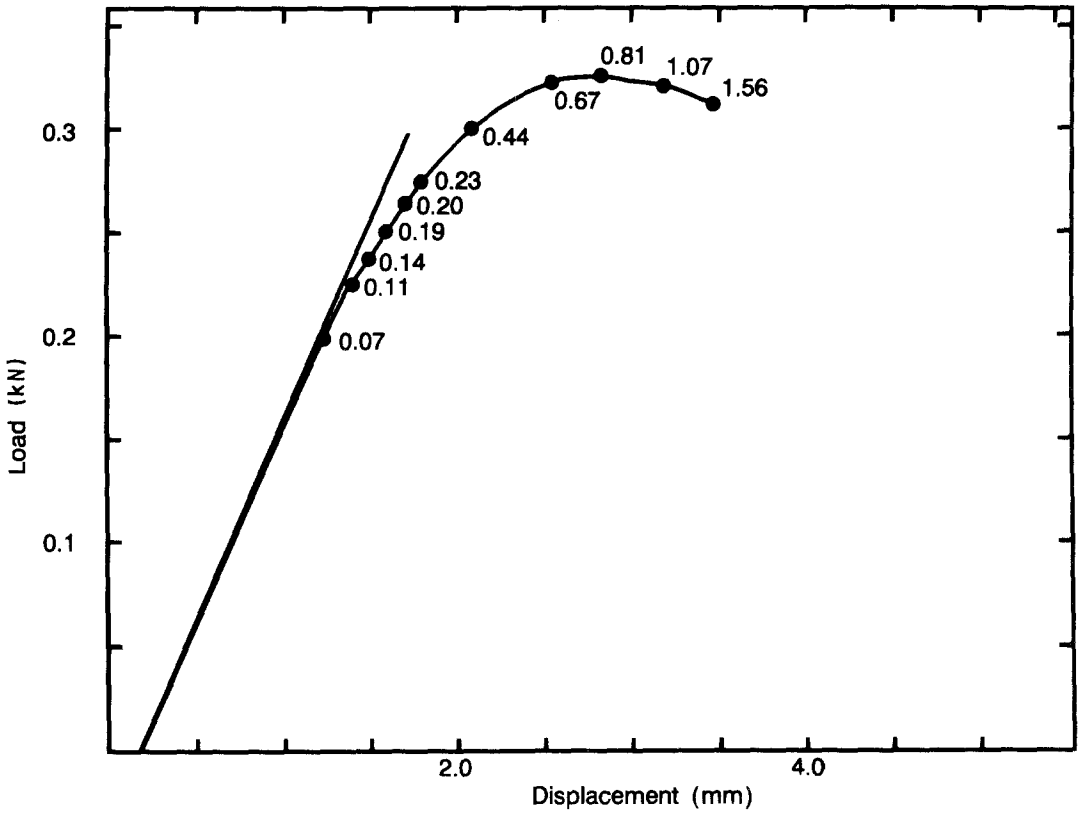

Figure 3 Load–deflection diagram and crack growth values for SENB specimens with width equal to 19.6 mm.

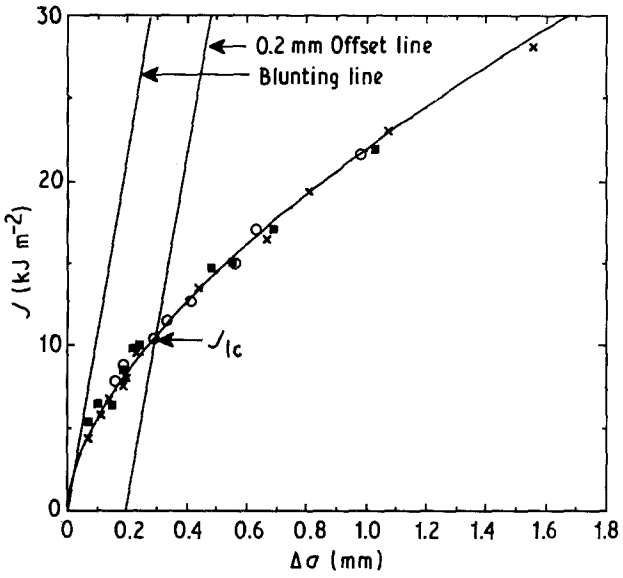

Figure 4 R-curve according to European Group on Fracture Task Group on Polymers protocol for J-testing of plastics. (○) W = 25.4 mm, (X) W = 19.6 mm, (■) W = 12.8 mm.

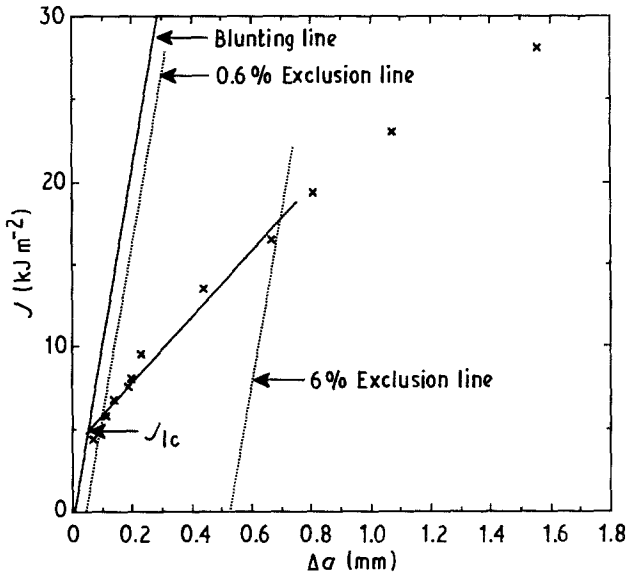

Figure 5 R-curve according to ASTME-813-81. (Specimen width equals 19.6 mm.)

by the two methods will be magnified if the R-curve is steeply rising, as is the case in this work.

Crack growth in the specimens used above occurred parallel to the mould-flow direction. To explore the possibility of anisotropy in the injection-molded plaques, a set of SENB specimens were machined so that crack growth would occur perpendicular to the mould-flow direction. The R-curve obtained from these specimens is shown in Fig. 6. It is evident from Fig. 6 that the direction of notching has no effect on the value of J_{Ic}. The effect of sidegrooving on the R-curve was also studied. Sidegrooves of equal depth were machined into each face of a specimen to give a total reduction in thickness of $0.2B$. The resulting R-curve, also shown in Fig. 6, is slightly higher than the R-curve for specimens without sidegrooves. The fracture surfaces of the sidegrooved specimens indicated that a small amount of crack growth originated at the sidegrooves, which may explain the slightly higher resistance curve for sidegrooved specimens.

An optical micrograph of a typical fracture surface is shown in Fig. 7a. The crack front is fairly straight except at the edges of the specimen where some curvature occurs. Also, a sharply defined whitened plastic

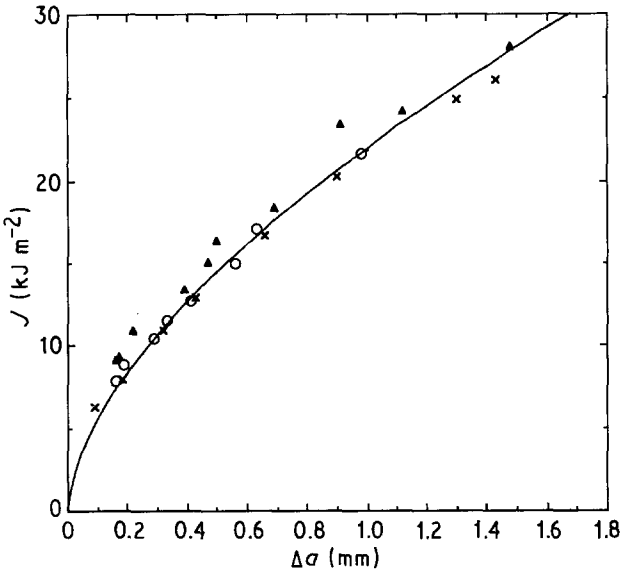

Figure 6 *R*-curve for specimens with sidegrooves (▲), crack growth parallel to mould-flow (X), crack growth perpendicular to mould-flow (○).

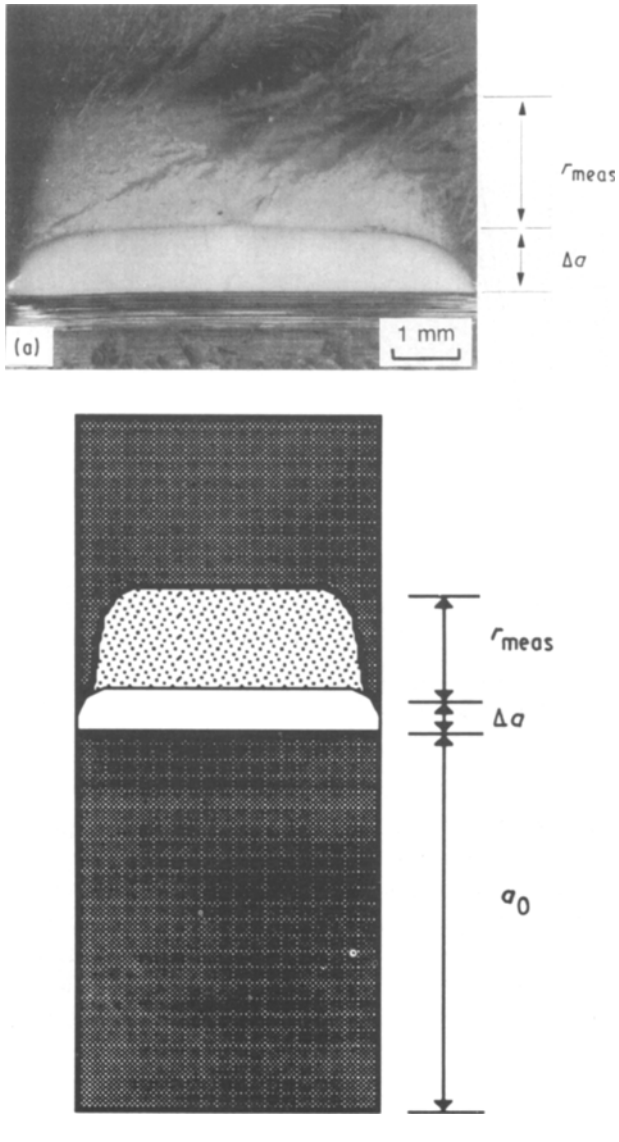

Figure 7 (a) Optical micrograph of a typical fracture surface. (b) Schematic diagram of a typical fracture surface.

zone ahead of the crack tip is clearly visible in the micrograph. (The blend contained a dark pigment which enhanced the contrast between the plastic zone and the unperturbed material.) This whitened plastic zone tapers inward as distance from the crack front increases, as shown schematically in Fib. 7b. In the plastic zone region the material at the edges of the specimen is not whitened indicating that the deformation mechanism which predominates in these regions differs from that in the whitened plastic zone. This may be caused by a transition from a plane strain stress state in the centre of a specimen to a plane stress stress state in the surface regions. The length of the plastic zone, r_{meas}, for each specimen shown in Fig. 3 was measured from an optical micrograph of the fracture surface. The values of r_{meas} are listed in Table I. It is clear from Table I that r_{meas} increases as Δa increases. Another feature of the whitened plastic zone is that the amount of tapering increases as r_{meas} increases. It should be noted that a specimen that had not been tested was cooled and broken open to determine if the whitened zone ahead of the crack tip is an artifact from the cooling and breaking open procedure. No whitened features were observed on the fracture surface of this specimen indicating that in the *J*-tests the whitened zone ahead of the crack tip formed during stable crack growth.

It was postulated earlier that a LEFM parameter could be used to characterize fracture in this material and in similar toughened materials because crack initiation occurred shortly after the onset of non-linearity. The stress intensity factor, K, for each of the specimens shown in Fig. 3 was calculated by using the relation

$$K = Y\sigma a^{1/2}$$

where Y is a geometry factor, and $a = a_0 + \Delta a$. These values of K are listed in Table I. The Dugdale analysis of the plastic zone predicts that the size of the plastic zone, r_p, ahead of a crack tip in an elastic body is given by

$$r_p = 0.393(K/m\sigma_y)^2 \quad (2)$$

where m is the plastic constraint factor. The values of r_p predicted by Equation 2 for $m = 1$, plane stress conditions, are listed in Table I. These values are consistently larger than the corresponding values of r_{meas}. However, if the added constraint from plane strain conditions is represented by assuming that $m = 3^{1/2}$[2], the calculated values or r_p agree quite well with r_{meas} up to a value of approximately 1.2 mm. Beyond 1.2 mm, the plane strain value of r_p is lower than r_{meas}. A larger contribution from plane stress at the larger values of K may explain this observation. This is supported by the fact that the larger plastic zones are more tapered than the smaller ones. Finally, the values of K shown in Table I were converted into values of J, assuming plane strain conditions, by using the relation:

$$J = K^2(1 - \nu^2)/E$$

where E is Young's modulus and ν is Poisson's ratio. These J values are plotted in Fig. 8. For $\Delta a < 0.3$ mm

TABLE I Evaluation of plastic zone size

Specimen	Δa (mm)	r_{meas} (mm)	K_c (MN m$^{-3/2}$)	$r_p(m = 1)$ (mm)	$r_p(m = 3^{1/2})$ (mm)	J (kJ m^{-2})
1	1.56	2.25	6.18	5.32	1.77	16.74
2	1.07	1.94	5.67	4.48	1.49	14.09
3	0.81	1.81	5.53	4.26	1.42	13.41
4	0.67	1.62	5.32	3.94	1.31	12.40
5	0.44	1.31	4.79	3.20	1.07	10.08
6	0.23	1.13	4.22	2.49	0.83	7.82
7	0.20	0.63	3.99	2.22	0.74	7.00
8	0.19	0.75	3.81	2.03	0.68	6.37
9	0.14	0.63	3.59	1.79	0.60	5.65
10	0.11	0.50	3.40	1.61	0.54	5.06
11	0.07	0.44	2.98	1.24	0.41	3.90

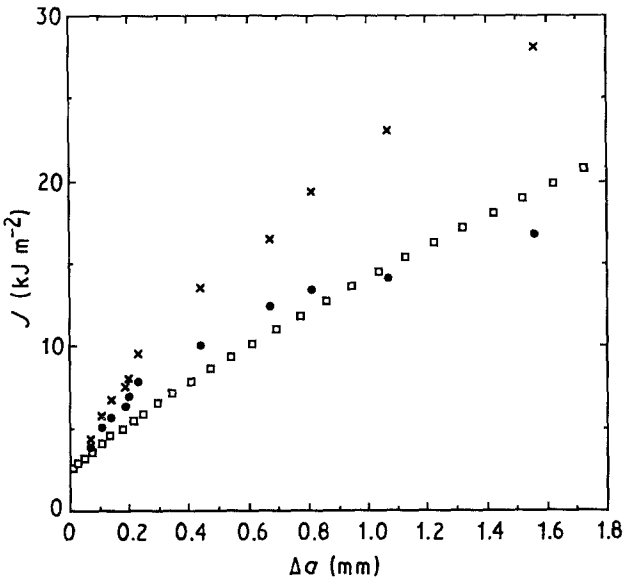

Figure 8 R-curves: values of a and J determined experimentally (X); values of a determined experimentally and values of J determined from K (●); values of a and J determined from a single load–deflection curve by compliance measurements assuming no plasticity (□).

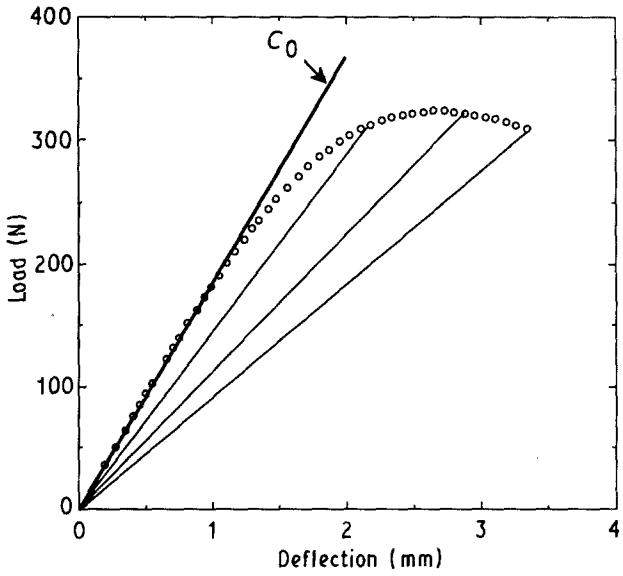

Figure 9 Compliance measurements from a typical load–deflection diagram.

the values of J calculated from K agree closely with the experimental values of J. Thus it appears that at least the initial stages of non-linearity in the load–deflection curve may be adequately described by LEFM.

Another approach to analysing this data with LEFM is to assume that no plasticity occurs in a specimen and that all of the non-linearity in the load–deflection diagram is due solely to crack growth. In this situation, Δa at any point along the load–deflection diagram can be determined from a compliance measurement. The energy calibration factor, Φ, in an elastic body is given by [1]:

$$\Phi = C/(W\mathrm{d}C/\mathrm{d}a) \quad (3)$$

where C is the compliance of the body. Since $(1\text{-}a/W)/\Phi \approx 2$ for SENB specimens with $S/W = 4$, Equation 3 becomes

$$\mathrm{d}a/(W - a) = 0.5\mathrm{d}C/C$$

Integrating gives

$$\Delta a = (W - a_0)(1 - (C_0/C)^{1/2}) \quad (4)$$

where C_0 is the compliance at $a = a_0$. Using Equation 4, Δa was calculated at discrete intervals along the load–deflection curve of a typical specimen, as illustrated in Fig. 9. An R-curve was constructed with these values of Δa and is compared to the experimentally determined R-curve in Fig. 8. At any particular value of J, the R-curve from compliance measurements predicts a larger value of Δa than was actually observed. This is not unexpected since the compliance approach attributes all non-linearity to crack growth. However, it is interesting to note that the R-curve from compliance measurements agrees quite well with the experimental R-curve at small values of Δa where plasticity would have the least effect, as suggested by the values of r_{meas} in Table I.

SEM micrographs of a typical fracture surface are shown in Fig. 10. In the region of slow crack growth (Fig. 10a) the matrix has yielded and voids appeared to have formed around the rubber particles. In a region of the fracture surface which is far removed from the plastic zone (Fig. 10c) the rubber particles are clearly visible and there is no evidence of voiding in or around the rubber particles. In the whitened plastic zone region (Fig. 10b) numerous holes, approximately the size of the rubber particles, have formed and only a

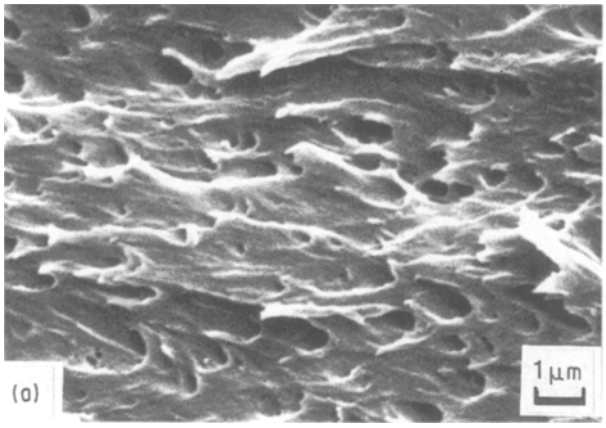

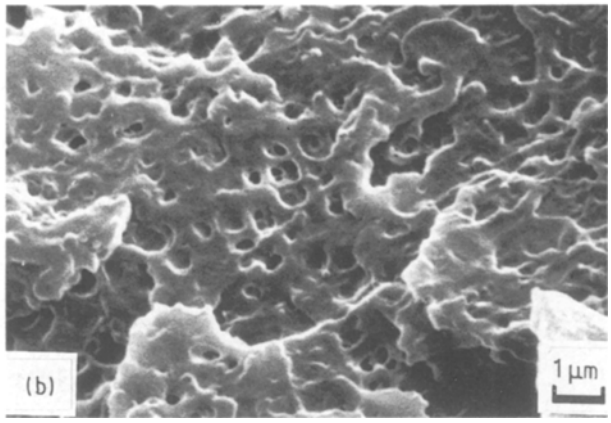

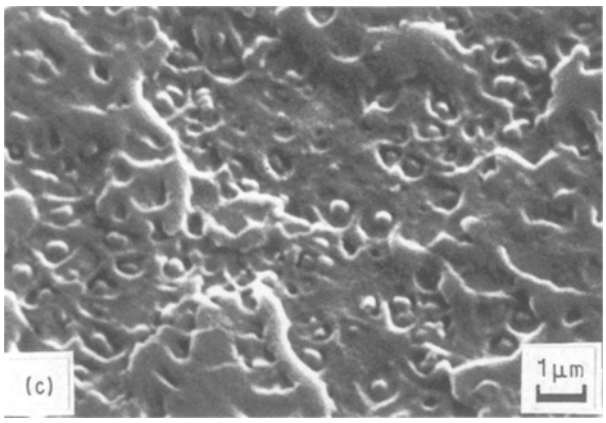

Figure 10 Scanning electron micrographs of (a) the slow growth region, (b) the whitened plastic zone region, and (c) a region of fast fracture far removed from the plastic zone. Crack growth occurs from right to left.

few rubber particles appear. These observations suggest that the rubber particles have debonded from the matrix. This debonding would relieve the unfavourable triaxial stress field in the centre of the material and allow the matrix to yield more easily.

Yee *et al.* [12] observed similar features on fracture surfaces of core-shell impact modified polycarbonate and suggested that the impact modifier may have debonded from the matrix. However, they concluded from subsequent studies of sectioned specimens that the core-shell impact modifer did not debond from the matrix but internally cavitated and thus relieved the triaxial stresses. An optical micrograph of a polished, sectioned specimen from this work is shown in Fig. 11. Surprisingly, there is no evidence of a plastic zone ahead of the crack tip, although a plastic zone is clearly indicated on the fracture surface (see Fig. 7a). There is evidence for some type of highly localized plastic deformation in the regions bordering the newly formed crack surfaces. An optical micrograph of a 25 μm thick microtomed section from the inner surface is shown in Fig. 12. Once again there is no clear evidence for plasticity ahead of the crack tip. These observations are in stark contrast to the observations of Yee *et al.* [12] and Narisawa and Takemori [7]. Both groups observed well-defined spherical or elliptical plastic zones in sectioned specimens. It is not clear at this time why similar features were not observed in the material used in this work, given its similarity to the materials used by Yee *et al.* [12] and by Narisawa and Takemori [7]. Transmission electron microscopy of microtomed sections is currently being conducted and will be reported in a subsequent paper.

4. Summary and conclusions

The fracture toughness of a toughened polycarbonate–copolyester blend was determined with the J-integral approach. A J_{1c} value of 10.8 kJ m^{-2} was obtained by using a protocol developed by the European Group on Fracture Polymer Task Group. A J_{1c} value of 4.9 kJ m^{-2} was obtained by using ASTM Standard E-813-81. The latter value agreed well with J_{1c} values obtained on similar materials in previous studies [7, 12]. Specimen width, mould-flow direction, and side-grooving did not affect the R-curve or value of J_{1c}.

The initiation of crack growth in the toughened blend occurred shortly after the onset of non-linearity in the load–deflection diagram. This suggested that LEFM could be used to characterize fracture toughness. From measurements of the plastic zone size it was shown that LEFM provided an adequate description of the initial stages of crack growth. Thus it appears that an engineering estimate of the material's resistance to crack initiation may be taken as the stress intensity factor at the onset of non-linearity in the load–deflection diagram, K_c'. K_c' for this blend is approximately equal to 3.0 MN m$^{-3/2}$. Since J-tests on

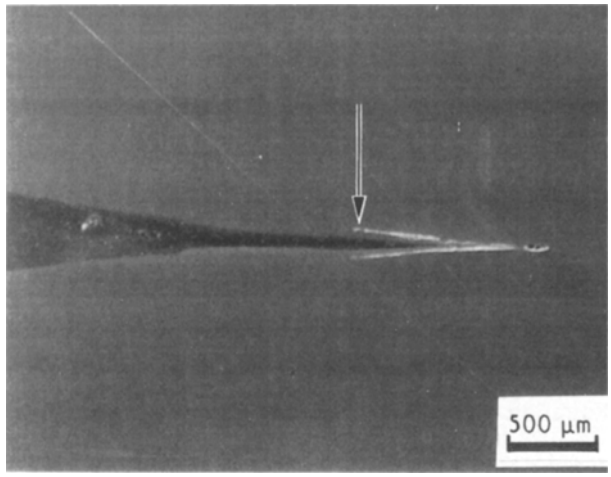

Figure 11 Optical micrograph of a polished section SENB specimen viewed under reflected light. The arrow indicates the tip of the precrack.

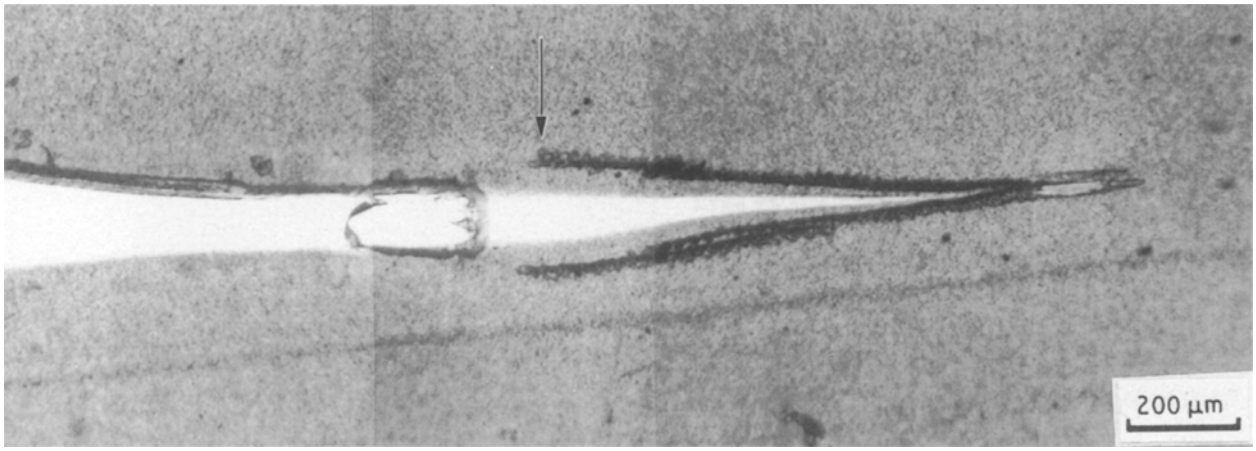

Figure 12 Optical micrograph of a 25 μm thick section from the crack tip region viewed with transmitted light. The arrow indicates the tip of the precrack.

many other rubber-toughened polymers showed that crack initiation occurs shortly after the onset of non-linearity, K_c' may provide a simple and effective estimate of fracture toughness for this class of material.

Finally, fractographic analyses suggested that the matrix has debonded from the core-shell impact modifier. This dilatational process would relieve the triaxial stresses and enhance shear yielding of the matrix. Further analysis is needed to determine if cavitation of the rubber particles occurs.

Acknowledgements

The author thanks Professor J. Gordon Williams, Imperial College, for his comments on the manuscript. The author also thanks R. McGill and L. Roberson for performing the microscopy analyses.

References

1. J. G. WILLIAMS, "Fracture mechanics of polymers" (Ellis Horwood, Chichester, 1987).
2. A. J. KINLOCH and R. J. YOUNG,"Fracture behavior of polymers" (Elsevier Applied Science, London, 1983).
3. ASTM Standard E-399-78, "Standard test method for plane strain fracture toughness of metallic materials" (American Society for Testing and Materials, Philadelphia, 1979) p. 540.
4. C. B. BUCKNALL, "Toughened plastics" (Applied Science Publishers, London, 1977).
5. J. A. BEGLEY and J. D. LANDES, in "Fracture toughness", ASTM STP 514 (American Society for Testing and Materials, Philadelphia, 1972) p. 1.
6. ASTM Standard E-813-87, "Standard test method for J_{Ic}, a measure of fracture toughness" (American Society for Testing and Materials, Philadelphia, 1987) p. 686.
7. I. NARISAWA and M. T. TAKEMORI, *Polym. Engng Sci.* **29** (1989) 671.
8. J. G. WILLIAMS and S. HASHEMI, *NATO ASI Ser.* E **89** (1985) 760.
9. S. HASHEMI and J. G. WILLIAMS, *Polym. Engng Sci.* **26** (1986) 760.
10. D. D. HUANG and J. G. WILLIAMS, *J. Mater. Sci.* **22** (1987) 2503.
11. S. HASHEMI and J. G. WILLIAMS, *Plastics Rubber Processing Applic.* **6** (1986) 363.
12. D. S. PARKER, H. -J. SUE, J. HUANG and A. F. YEE, *Polymer* **31** (1990) 2267.
13. G. E. HALE, "Crack growth resistance curves for polymers–development of a multiple specimen testing protocol" (Eighth European Conference on Fracture, Turin, Italy, 1990).
14. ASTM Standard E-813-81, "Standard test method for J_{Ic}, a measure of fracture toughness" (American Society for Testing and Materials, Philadelphia, 1981) p 810.

Received 9 May
and accepted 12 September 1991